

## Fugacity coefficients of hydrogen in (hydrogen + butane)

Thomas J. Bruno and Stephanie L. Outcalt

*Thermophysics Division, National Institute of Standards and Technology, Boulder, CO 80303, U.S.A.*

*(Received 2 November 1992; in final form 9 February 1993)*

The fugacity coefficients of hydrogen in (hydrogen + butane) were measured as a function of composition with a physical-equilibrium technique at (temperature, pressure) pairs of (433.15 K, 3.39 MPa), (473.15 K, 3.38 MPa), (473.15 K, 22.65 MPa), and (523.15 K, 3.42 MPa). The physical-equilibrium technique involved the use of an experimental chamber that was divided into two separate regions by a semipermeable membrane through which hydrogen, but not butane, could permeate. Measurement of the gas pressures on each side of the membrane, in addition to a measurement of the composition and the system temperature, allowed the calculation of the fugacity and fugacity coefficient of hydrogen in the mixture. The qualitative features of the measurements are discussed, and comparisons are made with predictions obtained from the Redlich–Kwong and Peng–Robinson models.

### 1. Introduction

The fugacity of individual components of a gaseous mixture can, in principle, be calculated from an applicable equation of state if the surface ( $p, V_m, T$ ) of the mixture is known in the region of interest along an isotherm with, for example:

$$\ln(f_i/x_i p) = \int_p^0 \{(V_i/RT) - (1/p)\} dp. \quad (1)$$

In equation (1),  $f_i$  is the fugacity of component  $i$ ,  $x_i$  is its mole fraction,  $V_i$  is its partial molar volume,  $p$  is the pressure of the mixture,  $T$  is the temperature, and  $R$  is the gas constant. The need for a great deal of accurate ( $p, V_m, T$ ) measurements for the mixture and the limitations inherent in many of the common equations of state can often make this approach time consuming and difficult. In the special case of gaseous mixtures containing hydrogen as one component, the physical-equilibrium method provides a great experimental simplification.<sup>(1)</sup> The problem of measuring the properties of a mixture is reduced to that of measuring the properties of a pure gas.

This work is part of an ongoing systematic investigation in which (hydrogen + methane or ethane or propane or 2-methylpropane or carbon dioxide or carbon monoxide or ammonia) have been studied.<sup>(2–10)</sup>

<sup>a</sup>Contribution of the United States Government. Not subject to copyright in the United States.

To implement the physical-equilibrium method for binary mixtures containing hydrogen as one component, an experimental chamber, usually a pressure vessel, is divided into two regions by a membrane that is permeable only to hydrogen. The membrane most often takes the form of long sections of thin-walled tubing of an appropriate material. If the volume on one side of the membrane is filled with the gaseous mixture, of which hydrogen is a component, and the volume on the other side is initially evacuated, hydrogen from the mixture will permeate through the membrane into the evacuated space. An equilibrium is eventually established between the gases separated by the membrane. The approach to equilibrium is driven by the need to equalize the chemical potentials of  $H_2$  on each side of the membrane barrier. When equilibrium is eventually reached, the fugacities of hydrogen on each side of the membrane must be equal.<sup>(11)</sup>

Appropriate instrumentation described more fully in previous papers<sup>(2-10)</sup> allows the pressure  $p^*(H_2)$  of the pure hydrogen that has permeated the membrane, and the pressure  $p$  of the binary mixture, to be measured at a given temperature  $T$ , and hydrogen mole fraction  $x$ . The superscript \* indicates a quantity describing a pure component. From these measurements, the fugacity of pure hydrogen can be computed. We can begin the computation (at moderate pressures) using the pressure expansion of the virial equation of state (truncated after the third virial coefficient):

$$\ln\{\phi^*(H_2)\} = (B/R)\{p(H_2)/T\} + (C - B^2)\{p(H_2)\}^2/2R^2T^2, \quad (2)$$

where  $B$  and  $C$  are the second and third virial coefficients, respectively, and  $\phi^*(H_2)$  is the fugacity coefficient of pure hydrogen (that has permeated from outside the membrane). The virial coefficients for hydrogen are well known,<sup>(12-14)</sup> and the virial equation has been found to provide fugacities of adequate accuracy at the pressures and temperatures encountered in this work. The use of a numerical integration of the measured ( $p$ ,  $V_m$ ,  $T$ ) surface would not necessarily improve the overall accuracy of the fugacity coefficient since the largest source of error is the measurement of  $x$ .<sup>(2)</sup> The fugacity  $f^*(H_2)$  of the pure hydrogen follows from

$$f^*(H_2) = \phi^*(H_2)p^*(H_2). \quad (3)$$

Since the measurements are performed after the system has reached equilibrium (that is, after there is no net change in pressure with time on either side of the membrane, with the temperature of the system held constant), the fugacities of hydrogen in the volumes on both sides of the membrane must be equal. The fugacity coefficient of hydrogen in the mixture can then be obtained from

$$f^*(H_2) = f(H_2) = xp\phi(H_2). \quad (4)$$

In equation (4),  $f(H_2)$  and  $\phi(H_2)$  are the fugacity and fugacity coefficient, respectively, of hydrogen in the mixture. The mole fraction of hydrogen given in equation (4) is measured after the permeation through the membrane has occurred, and equilibrium has been reached. The mixture pressure  $p$  is maintained constant within experimental error for each measured  $\{\phi(H_2), x\}$  pair. The presentation of the experimental results is thus a plot of  $\phi(H_2)$  against  $x$  at a given temperature and mixture pressure.

## 2. Experimental

The apparatus used in this work was essentially the same as that used in previous studies.<sup>(2-10)</sup> Two notable modifications were made to the apparatus. Firstly, the pressure vessel was surrounded on all sides by an aluminum shield with a thickness of 1.8 cm. The shield was not in contact with the vessel, but rather was offset by an air space of approximately 1 cm. The purpose of this shielding was to provide temperature uniformity along the entire length of the vessel. Secondly, the transfer lines and valve manifold required for sampling and pressure measurements were resistively heated to prevent fluid condensation.

The mole fractions  $x(\text{H}_2)$  in the mixtures studied were determined by means of a chromatographic method applied with a developmental g.c. that was specially constructed for gas analysis. A packed column of Porapak-QS† (2 m in length, 0.32 cm in diameter), of 105  $\mu\text{m}$  to 74  $\mu\text{m}$  particle size provided the separation. Although mass-balance methods appear attractive because of the ability to prepare a mixture gravimetrically to an accuracy approaching mass fraction  $1 \cdot 10^{-10}$ , several factors make this approach impractical. The main factor is that mass-balance calculations require a measure of the absolute volume of the membrane and associated transfer lines and valving. Under the influence of temperature and pressure, this volume can change by as much as 19 per cent over the conditions of an entire series of measurements. The changes are not predictable or reproducible due to hysteresis effects and the stretching and twisting movements of the membrane tube and internal supporting spring.

Nitrogen was used as the chromatographic carrier gas at a volumetric flow rate of  $0.5 \text{ cm}^3 \cdot \text{s}^{-1}$ . Detection was provided by a thermal-conductivity detector that had a cell temperature of 318.15 K and a wire current of 200 mA. Sample introduction was done using a specially designed valve-based gas-sample injector.<sup>(16)</sup> The detector response was calibrated by the external-standard method with the pure components of the mixture and three gravimetrically prepared standard mixtures. The analyses were done isothermally at a column temperature of 318.15 K. The separation obtained under these conditions was very favorable to precise quantitation. In this respect, baseline-resolved peaks of experimentally convenient widths, convenient retention times, and excellent symmetry were easily obtained. The accuracy of  $x$  obtained from the analysis was approximately  $\pm 5 \cdot 10^{-3} \cdot x$  for  $\{x\text{H}_2 + (1-x)\text{CH}_3(\text{CH}_2)_2\text{CH}_3\}$  with  $x = 0.5$ .<sup>(2)</sup> Somewhat lower precision and accuracy were obtained at lower values of  $x$ .

The hydrogen used in this work was research grade and had a stated mass fraction of 0.99995. Analysis by low-temperature g.c. confirmed this purity and, therefore, the material was used with no further purification. The butane was also research grade, with a stated mass fraction of 0.999. Upon analysis by g.c., no major impurities were found, and the butane was used without further purification.

† Certain commercial equipment, instruments, or materials are identified in this paper in order to specify adequately the experimental procedure. Such identification does not imply recommendation or endorsement by the National Institute of Standards and Technology, nor does it imply that the materials or equipment that are identified are the best available for the purpose.

TABLE 1. Fugacity coefficients  $\phi(\text{H}_2)$  of hydrogen in  $\{x\text{H}_2 + (1-x)\text{CH}_3(\text{CH}_2)_2\text{CH}_3\}$ ;  $p^*(\text{H}_2)$  denotes the pressure of pure hydrogen which has permeated the membrane

$p^*(\text{H}_2)/\text{MPa}$	$x$	$\phi(\text{H}_2)$	$p^*(\text{H}_2)/\text{MPa}$	$x$	$\phi(\text{H}_2)$	$p^*(\text{H}_2)/\text{MPa}$	$x$	$\phi(\text{H}_2)$
$T = (433.16 \pm 0.01) \text{ K}; p = (3.39 \pm 0.07) \text{ MPa}$								
1.56	0.360	1.284	2.43	0.676	1.074	3.02	0.887	1.018
1.67	0.401	1.239	2.48	0.694	1.068	3.05	0.900	1.014
1.81	0.451	1.194	2.53	0.711	1.063	3.18	0.945	1.008
2.22	0.598	1.106	2.65	0.755	1.044	3.23	0.964	1.006
2.28	0.621	1.094	2.72	0.780	1.046	3.33	0.999	1.004
$T = (473.15 \pm 0.01) \text{ K}; p = (3.38 \pm 0.05) \text{ MPa}$								
1.59	0.429	1.099	2.44	0.708	1.027	2.96	0.882	1.006
1.81	0.503	1.073	2.53	0.740	1.023	3.05	0.910	1.002
1.59	0.548	1.058	2.62	0.768	1.019	3.20	0.963	0.996
1.99	0.563	1.052	2.69	0.790	1.016			
2.08	0.592	1.048	2.76	0.815	1.013			
$T = (473.15 \pm 0.01) \text{ K}; p = (22.65 \pm 0.15) \text{ MPa}$								
12.71	0.452	1.306	17.23	0.673	1.215	20.36	0.837	1.164
13.96	0.511	1.275	17.89	0.707	1.204	21.02	0.872	1.155
15.15	0.570	1.240	18.85	0.757	1.186			
16.01	0.611	1.235	19.58	0.795	1.176			
$T = (523.15 \pm 0.01) \text{ K}; p = (3.42 \pm 0.02) \text{ MPa}$								
2.39	0.703	1.004	2.61	0.771	1.000	2.96	0.893	0.981
2.57	0.756	1.003	2.85	0.853	0.989			

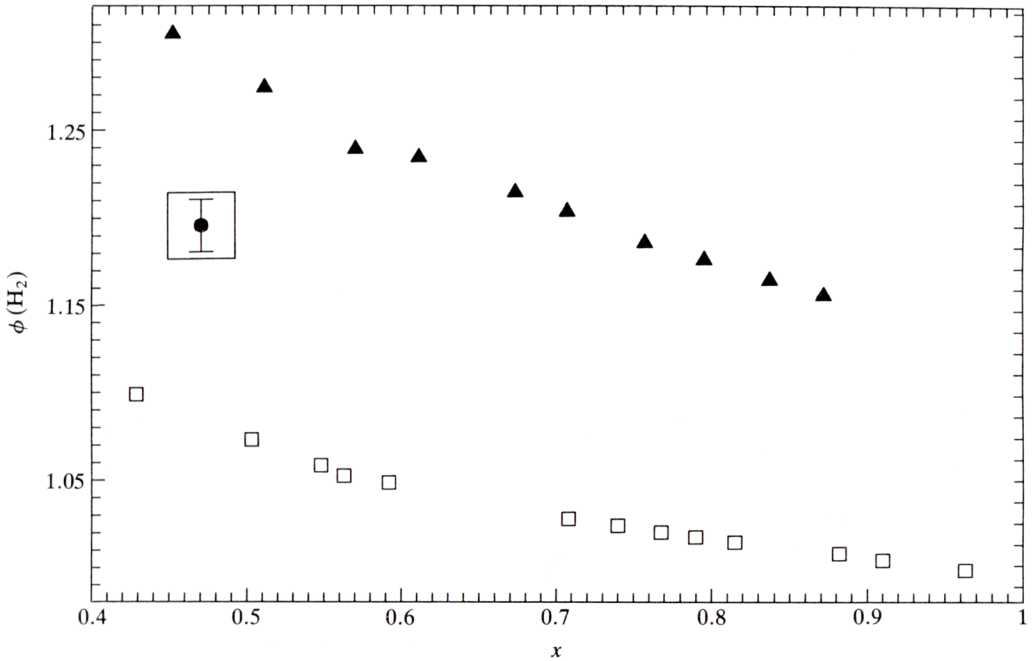


FIGURE 1. A plot of the fugacity coefficient  $\phi(\text{H}_2)$  against  $x$  for  $\{x\text{H}_2 + (1-x)\text{CH}_3(\text{CH}_2)_2\text{CH}_3\}$ . The measurements were performed at a nominal temperature of 473.15 K (see the table 1 subheadings for the measured values) and pressures:  $\square$ ,  $p = 3.38 \text{ MPa}$ ;  $\blacktriangle$ ,  $p = 22.65 \text{ MPa}$ . The error bar enclosed in the box represents the uncertainty of a  $\{\phi(\text{H}_2), x\}$  pair for  $\{0.5\text{H}_2 + 0.5\text{CH}_3(\text{CH}_2)_2\text{CH}_3\}$ .

### 3. Results and discussion

The fugacity coefficients  $\phi(\text{H}_2)$  of hydrogen and the measured values of  $x$  in  $\{x\text{H}_2 + (1-x)\text{CH}_3(\text{CH}_2)_2\text{CH}_3\}$  at (temperature, pressure) pairs of (523.15 K, 3.42 MPa), (433.15 K, 3.39 MPa), (473.15 K, 22.65 MPa), and (473.15 K, 3.38 MPa) are presented in table 1. The actual measured values of the temperature are presented in the table subheadings. The errors quoted in the table were determined from repeated measurements of temperature and pressure. A plot of the measured fugacity coefficients of hydrogen against  $x$  for the measurements performed at  $T = 473.15$  K is presented in figure 1. A plot of the measured fugacity coefficients of hydrogen against  $x$  for the measurements performed at  $p \approx 3.38$  MPa is presented in figure 2. The error bars enclosed in the boxes on these figures represent the uncertainty of a  $\{\phi(\text{H}_2), x\}$  pair for  $\{0.5\text{H}_2 + 0.5\text{CH}_3(\text{CH}_2)_2\text{CH}_3\}$ . This error is typically about  $0.015 \cdot \phi(\text{H}_2)$ . A detailed error-propagation analysis that described how the magnitude of this uncertainty was estimated has been presented previously.<sup>(2)</sup>

Some general qualitative statements can be made about the appearance of the measurements presented in figure 1. The change in  $\phi(\text{H}_2)$  with  $x$  is more pronounced

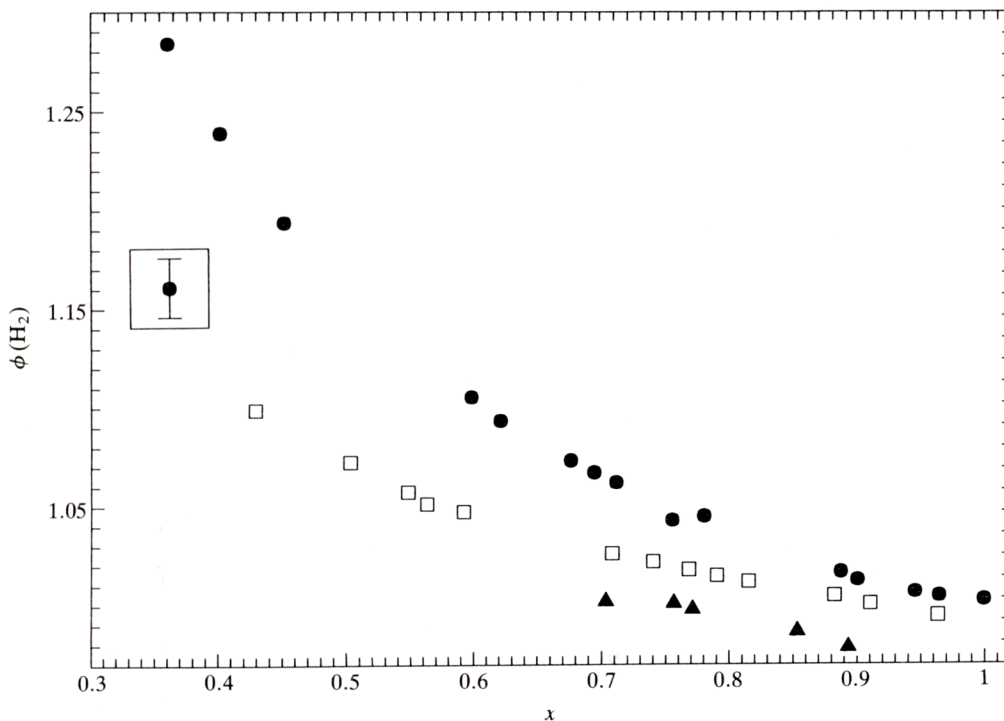


FIGURE 2. A plot of the fugacity coefficient  $\phi(\text{H}_2)$  against  $x$  for  $\{x\text{H}_2 + (1-x)\text{CH}_3(\text{CH}_2)_2\text{CH}_3\}$ . The measurements were performed at a nominal pressure of 3.39 MPa (see the table 1 subheadings for the measured values) and temperatures: ●,  $T = 433.15$  K; □,  $T = 473.15$  K; ▲,  $T = 523.15$  K. The error bar enclosed in the box represents the uncertainty of a pair for  $\{0.5\text{H}_2 + 0.5\text{CH}_3(\text{CH}_2)_2\text{CH}_3\}$ .

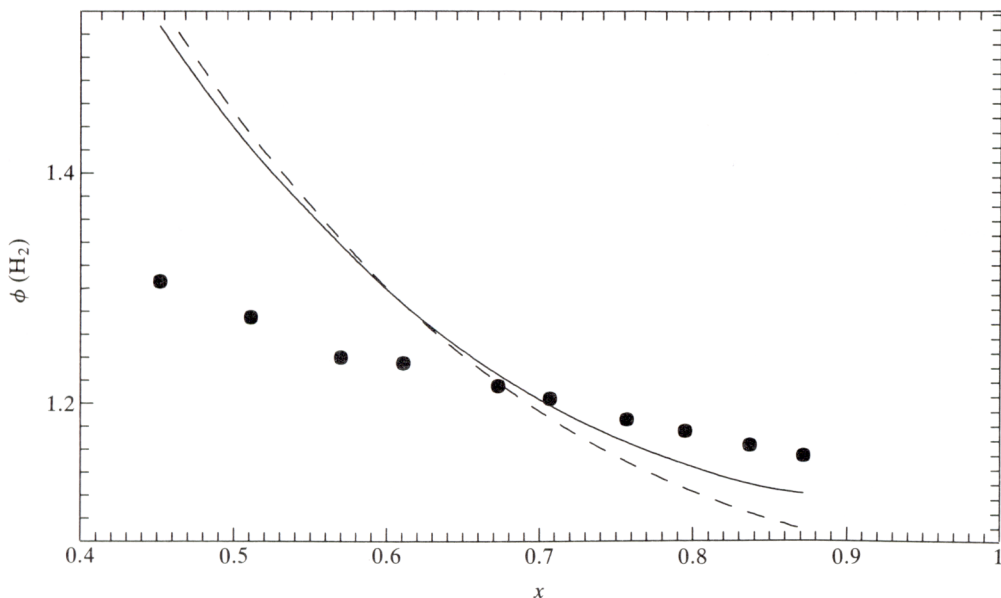


FIGURE 3. A plot of the fugacity coefficient  $\phi(\text{H}_2)$  against  $x$  for  $\{x\text{H}_2 + (1-x)\text{CH}_3(\text{CH}_2)_2\text{CH}_3\}$  at  $T = 473.15 \text{ K}$  and  $p = 22.65 \text{ MPa}$ . —, Predictions from the Redlich-Kwong equation; ---, predictions from the Peng-Robinson equation; ●, experimental measurements.

at lower values of  $x$ , with a gradual leveling off at the higher values. This observation is consistent for a gas of relatively low molar mass (above its critical temperature) in a mixture with a gas having a significantly higher molar mass. This behavior is predicted by most equations of state and has been observed in all mixtures studied by this method.<sup>(2-10)</sup> Unfortunately, limitations in the fluid-delivery manifold of the experimental apparatus prevented measurements from being obtained at  $x < 0.40$ . We are therefore unable to comment on the possible structure of the curves below this value.

The magnitudes of the individual  $\phi(\text{H}_2)$  values are also worthy of mention, since they are strongly dependent on the chemical nature of the mixture components. The  $\phi(\text{H}_2)$  values for (hydrogen + butane) are, in general, higher for a given  $x$  than those measured for the other mixtures that have been studied. This includes (hydrogen + 2-methylpropane).<sup>10</sup> These observations are consistent with equation-of-state predictions for a gas of low molar mass at a relatively high reduced temperature in a binary mixture with a heavier gas above its normal boiling temperature. It is also consistent with measurements performed by others<sup>(17)</sup> on this mixture at lower temperatures. We are currently formulating a general (fluid-independent) predictive procedure for  $\phi(\text{H}_2)$  values that is based upon the reduced temperature of the component mixed with hydrogen.

Figure 1 shows that, at constant temperature, an increase in the pressure of a mixture at a given  $x$  results in an increase in  $\phi(\text{H}_2)$ . This increase is reflected not only

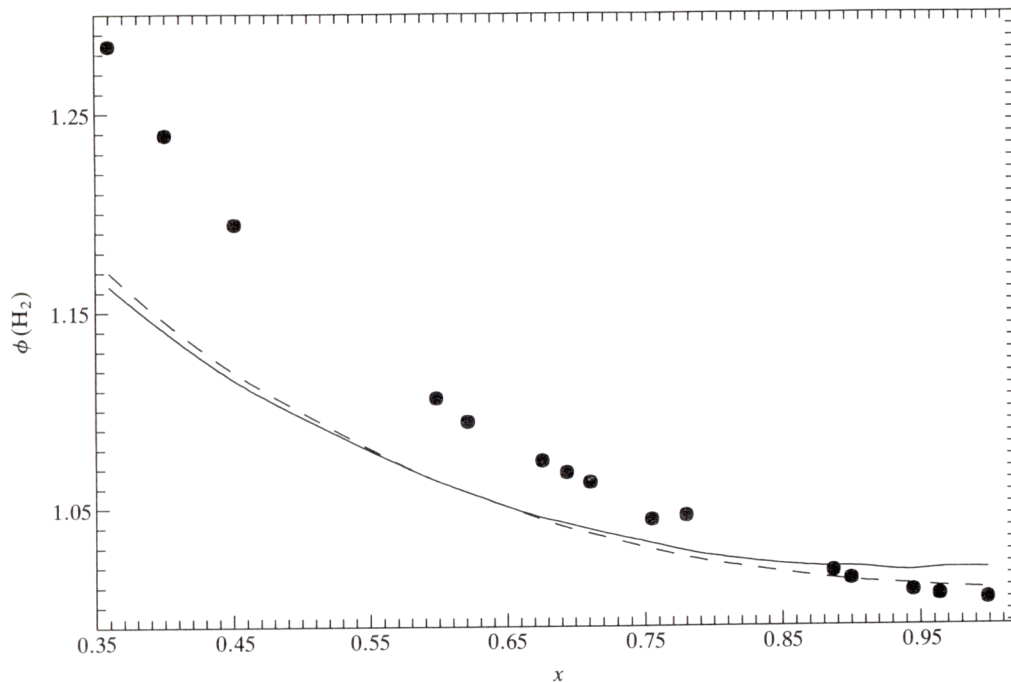


FIGURE 4. A plot of the fugacity coefficient  $\phi(\text{H}_2)$  against  $x$  for  $\{x\text{H}_2 + (1-x)\text{CH}_3(\text{CH}_2)_2\text{CH}_3\}$  at  $T = 433.15 \text{ K}$  and  $p = 3.42 \text{ MPa}$ . —, Predictions from the Redlich-Kwong equation; - - -, predictions from the Peng-Robinson equation; ●, experimental measurements.

in the values of the fugacity coefficients, but also in the rate of increase or slope of the curves. This observation is not surprising, since a higher degree of non-ideality is expected in the mixture at the higher pressure, and this is reflected in a higher value for the fugacity coefficient.

Figure 2 shows that, at constant total pressure of the mixture, a decrease in temperature results in an increase in  $\phi(\text{H}_2)$ . As with the isothermal measurements shown in figure 1, the increase in  $\phi(\text{H}_2)$  is seen in the increasing slope as a function of  $x$ .

In each of figures 3 through 6, the experimental measurements, the predictions of the Redlich-Kwong equation of state, and the predictions of the Peng-Robinson equation of state are shown. Van der Waals mixing rules have been used throughout. In the calculations presented in figures 3 through 6 with the Peng-Robinson equation, the acentric factor  $\omega$  was assigned a value of  $-0.22$  for  $\text{H}_2$ . Binary interaction coefficients were also assigned values of 0 for these predictions, since none are available in the temperature range of this work, and the measurements made in this study are not considered extensive enough to permit such coefficients to be determined.

Despite their inherent simplicity, both the Redlich-Kwong and Peng-Robinson equations of state provide reasonable predictions, within  $1.5 \cdot 10^{-2} \cdot \phi(\text{H}_2)$  to

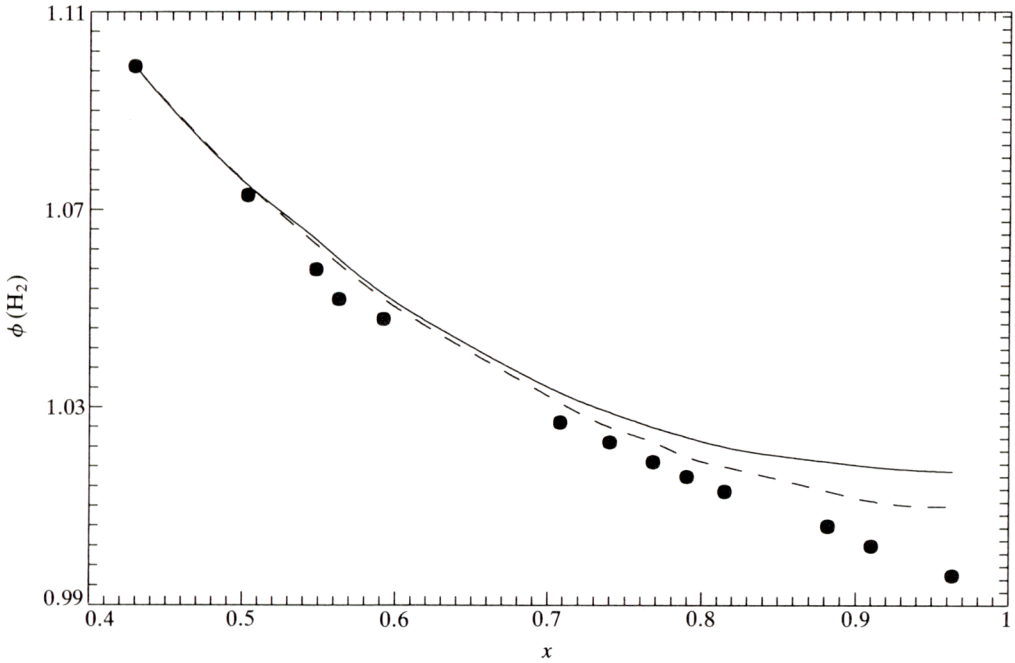


FIGURE 5. A plot of the fugacity coefficient  $\phi(\text{H}_2)$  against  $x$  for  $\{x\text{H}_2 + (1-x)\text{CH}_3(\text{CH}_2)_2\text{CH}_3\}$  at  $T = 473.15 \text{ K}$  and  $p = 3.38 \text{ MPa}$ . —, Predictions from the Redlich-Kwong equation; ---, predictions from the Peng-Robinson equation; ●, experimental measurements.

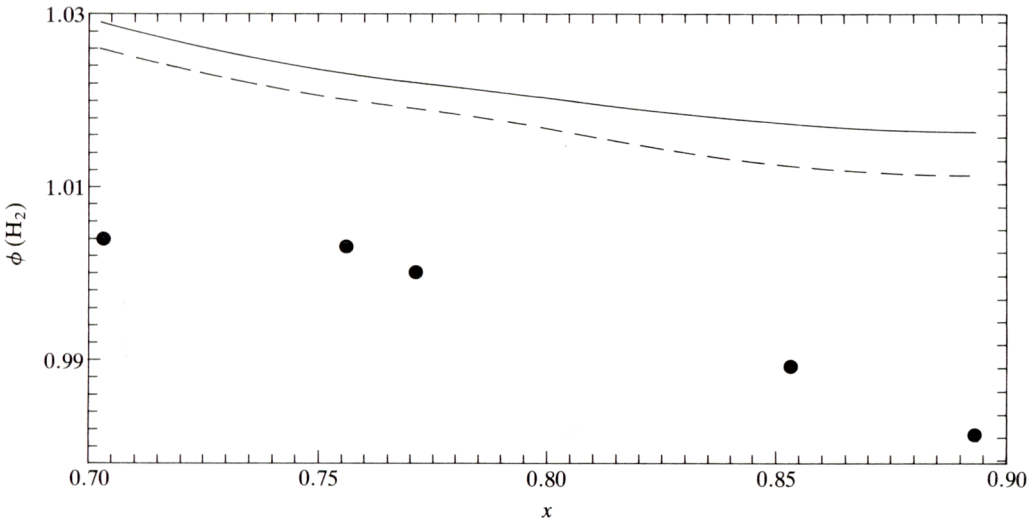


FIGURE 6. A plot of the fugacity coefficient  $\phi(\text{H}_2)$  against  $x$  for  $\{x\text{H}_2 + (1-x)\text{CH}_3(\text{CH}_2)_2\text{CH}_3\}$  at  $T = 523.15 \text{ K}$  and  $p = 3.42 \text{ MPa}$ . —, Predictions from the Redlich-Kwong equation; ---, predictions from the Peng-Robinson equation; ●, experimental measurements.

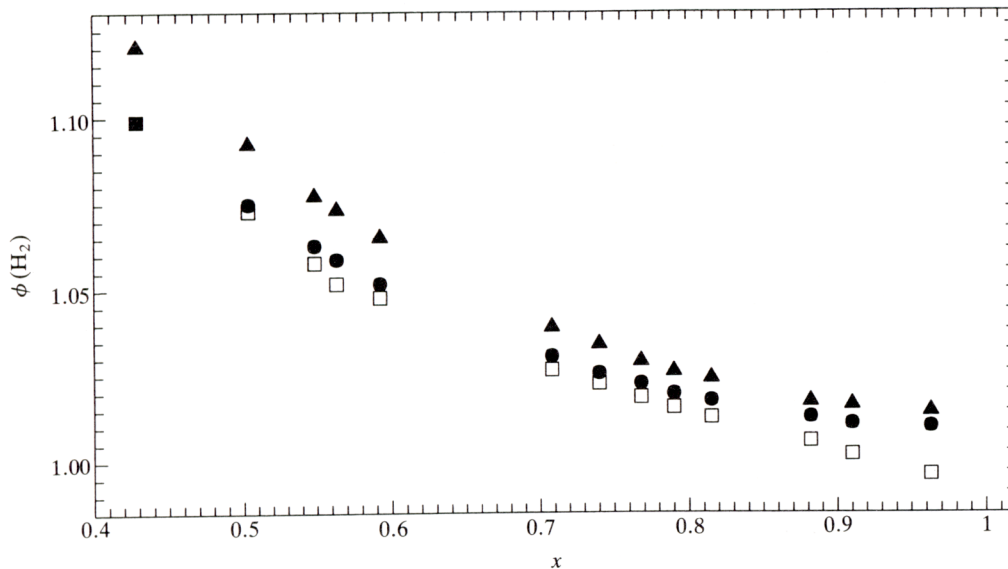


FIGURE 7. A plot of the measured fugacity coefficient  $\phi(\text{H}_2)$  against  $x$  for  $\{x\text{H}_2 + (1-x)\text{CH}_3(\text{CH}_2)_2\text{CH}_3\}$  and predictions of the fugacity coefficient obtained from the Peng–Robinson equation of state (with two values for the acentric factor  $\omega$ ) at  $T = 473.15$  K, and  $p = 3.38$  MPa.  $\blacktriangle$ , Calculated with  $\omega = 0$ ;  $\square$ , calculated with  $\omega = -0.22$ ;  $\bullet$ , experimental results.

$3 \cdot 10^{-2} \cdot \phi(\text{H}_2)$  in the region of  $x > 0.75$ . At lower  $x$ , the deviations of the predicted from the measured values generally become much greater. As expected, the equations of state provide better predictions at lower pressures (therefore, lower densities) for a given temperature over the range of  $x$  studied. In addition, predictions are better at higher temperatures. The reason for the apparent crossover from negative deviations (at high pressure, high temperature) to positive deviations (at low pressure, low temperature) is not known, and is the subject of current investigation.

The relatively poor agreement at lower values of  $x$  has been observed in all studies of this type.<sup>(2-10)</sup> At least part of the reason for the larger deviations can be ascribed to the more difficult experimental conditions in this range of  $x$ . The time required to achieve pressure equilibration on both sides of the membrane is much longer, and one can expect a slightly higher uncertainty in the pressure. In addition, the analytical conditions are slightly less favorable due to the smaller chromatographic peaks obtained for hydrogen. These differences in the experimental conditions are relatively minor, however, and are not sufficient to explain the difference in fugacity coefficients. Predicted values were also calculated with an extended-corresponding-states approach,<sup>(18)</sup> but these gave even larger deviations from the measured values and are not reported here.

The effect of  $\omega$  for hydrogen on the predicted values of  $\phi(\text{H}_2)$  obtained from the Peng–Robinson equation of state is pronounced. This observation has been made for all mixtures studied in the course of work with this apparatus.<sup>(2-10)</sup> In figure 7, the measurements taken at  $p = 3.38$  MPa and  $T = 473.15$  K are replotted to illustrate

the difference with  $\omega(\text{H}_2) = 0$  and with  $\omega(\text{H}_2) = -0.22$  (obtained from vapor-pressure measurements).<sup>(19)</sup>

The effect of this parameter change on the experimental value is to lower the predictions of the hydrogen fugacity coefficients in the mixture by  $1 \cdot 10^{-2} \cdot \phi(\text{H}_2)$  to  $2 \cdot 10^{-2} \cdot \phi(\text{H}_2)$ . With many fluids, the predicted values can sometimes drop below the measured values at  $0.7 \leq x \leq 0.75$ , and rise above the measurements at lower values of  $x$ . In the present case, the crossover occurs at a lower  $x$ , closer to  $x = 0.5$ . A scheme to parameterize the acentric factor using  $x$  is currently under development and will be reported later.

The financial support of the Gas Research Institute is gratefully acknowledged.

## REFERENCES

1. Cheh, H. Y. *Proc. 6th Symp. Thermophys. Props.* ASME: New York. **1973**, 256.
2. Bruno, T. J. *J. Res. Natl. Bur. Stand. (U.S.)* **1985**, 90, 127.
3. Bruno, T. J.; Hume, G. L.; Ely, J. F. *Int. J. Thermophys.* **1986**, 7, 1033.
4. Bruno, T. J.; Hume, G. L. *Int. J. Thermophys.* **1986**, 7, 1053.
5. Bruno, T. J. *Int. J. Thermophys.* **1987**, 8, 205.
6. Bruno, T. J.; Schroeder, J. A. *Int. J. Thermophys.* **1987**, 8, 437.
7. Bruno, T. J.; Schroeder, J. A. *Int. J. Thermophys.* **1988**, 9, 525.
8. Bruno, T. J.; Outcalt, S. L. *Int. J. Thermophys.* **1990**, 11, 109.
9. Bruno, T. J.; Schroeder, J. A.; Outcalt, S. L. *Int. J. Thermophys.* **1990**, 11, 889.
10. Bruno, T. J.; Outcalt, S. L. *J. Chem. Thermodynamics* **1990**, 22, 873–883.
11. Prausnitz, J. M.; Lichenthaler, R. N.; de Azevedo, E. G. *Molecular Thermodynamics of Fluid Phase Equilibria*. 2nd edition. Prentice-Hall: Englewood Cliffs, NJ. **1985**.
12. Levelt Sengers, J. M. H.; Klein, M.; Gallagher, J. S. *Report AEDC-TR-71-39, USAF*. **1971**.
13. Goodwin, R. D. (NIST) Personal communication, 1984.
14. McCarty, R. D. (NIST) Personal communication, 1984.
15. *ASME Boiler and Pressure Vessel Code. Sec. VIII: Unfired Pressure Vessels*. ASME: New York. **1965**.
16. Bruno, T. J. *J. Chromatogr. Sci.* **1985**, 23, 325.
17. Klink, A. E.; Cheh, H. Y.; Amick, E. H. *AIChE J.* **1975**, 21, 1142.
18. Ely, J. F. *Proc. 63rd Gas Process. Assoc. Conv.* Tulsa, OK. **1984**, p. 9.
19. Reid, R. C.; Prausnitz, J. M.; Poling, B. E. *The Properties of Gases and Liquids*. 4th edition. McGraw-Hill: New York. **1987**.